CR 115511

OPTIMIZATION OF A FLUIDIC TEMPERATURE CONTROL DEVICE

C1

December 1970

Prepared under Contract No. NAS 9-10858

by

Honeywell Inc.

Systems and Research Division

Minneapolis, Minnesota 55113

for

National Aeronautics and Space Administration

OPTIMIZATION OF A FLUIDIC TEMPERATURE CONTROL DEVICE

by

J. M. Zabsky
D. R. Rask
J. B. Starr

December 1970

Prepared under Contract No NAS 9-10858 by

Honeywell Inc.
Systems and Research Division
Minneapolis, Minnesota 55113

for

NATIONAL AERONAUTICS AND SPACE ADMINISTRATION

FOREWORD

This report documents work performed during a seven-month experimental effort by Honeywell's Systems and Research Center under NASA Contract NAS 8-10858, "Optimization of a Fluidic Control System." The authors wish to acknowledge the guidance and contributions given to this program by the technical monitor, Mr. Steve Martin, NASA Manned Spacecraft Center, Houston, Texas.

CONTENTS

ILLUSTRATIONS

OPTIMIZATION OF A FLUIDIC TEMPERATURE CONTROL DEVICE

By J. M. Zabsky
D. R. Rask
J. B. Starr

SUMMARY

Controlling heat rejection in liquid-cooled space suits without having to bypass the liquid flow around the garment demands a controller that produces a large range of coolant temperatures. This program refined an existing fluidic temperature control system developed under a prior study which modulated temperature at the inlet to the liquid-cooled garment by using existing liquid supply and return lines to transmit signals to a fluidic controller located in the spacecraft. This earlier system produced a limited range of garment inlet temperatures, requiring some bypassing of flow around the suit to make the astronaut comfortable at rest conditions.

Refinements were mostly based on a flow visualization study of the key element in the fluidic controller: the fluidic mixing valve. The valve's mixing-ratio range was achieved by making five key changes: 1) geometrical changes to the valve; 2) attenuation of noise generated in proportional amplifier cascades; 3) elimination of vortices at the exit of the fluidic mixing valve; 4) reduction of internal heat transfer; and 5) flow balancing through venting. As a result, the refined system is now capable of modulating garment inlet temperature from 45°F to 70°F with a single manual control valve in series with the garment. This control valve signals without changing or bypassing flow through the garment.

INTRODUCTION

Under contract NAS 9-8249, Honeywell developed a fluidic control system that modulates coolant temperature at the inlet of a liquid-cooled garment connected to a spacecraft by an umbilical. To eliminate adding electrical or hydraulic lines, temperatures are modulated by signals transmitted through existing liquid supply and return conduits. The system modulates coolant temperature in response to changes in pressure drop across the liquid-cooled garment. Modulation takes place within a fluidic temperature controller, which could be located within the spacecraft. The controller contains no moving parts and responds to pressure signal differentials of less than 0.1 inch of water.

Heart of the controller is a fluidic mixing valve developed under the contract. This valve modulates the mixture ratio of cold water flow to total garment flow over the range 0.1 to 0.9. In general, the mixture ratio of 0.9 lowers temperatures enough for adequate cooling; however, the 0.1 lower limit of the mixture ratio limits the minimum cooling rate to about 700 BTU's per hour. Thus, when the subject is resting and his metabolic rate is lower than 400 BTU's per hour, cooling is excessive. A temporary solution has been to use flow modulation by routing the coolant around the liquid-cooled garment through a bypass. Such bypassing, however, somewhat increases the complexity of the manual control valve.

Through flow visualization experiments, the fluidic mixing valve can be designed to broaden the range of mixture ratios, thus reducing the lower cooling limit of the system. Such experiments show flow patterns within the fluidic device, thereby suggesting changes in device geometry to extend mixture ratio range.

Presented herein are the results of such a study to improve controller performance, thus increasing the range of garment inlet temperatures. Controller refinements resulted from changing mixing valve geometry, reducing noise, balancing flow, and reducing heat transfer. The refined system can deliver water temperatures ranging from 45°F to 70°F. A single, manually controlled valve modulates temperature without bypassing or reducing flow through the garment.

EXISTING SYSTEM DESCRIPTION

The existing fluidic temperature control of liquid-cooled space suits was developed under NASA Contract No. NAS 9-8249. Reference 1 fully describes the control system analysis, fabrication details, and performance. The system modulates coolant temperature at the inlet of a liquid-cooled garment connected to a spacecraft by an umbilical. Temperature modulation occurs in response to sensed changes in pressure drop across the garment. All control signals are transmitted through existing liquid supply and return conduits to a fluidic temperature controller located in the spacecraft. The no-moving-parts controller responds to pressure-difference signals of less than 0.1 inch of water and modulates temperature through a fluidic mixing valve. A special manual control circuit located at the garment permits selecting three different levels of cooling. The manual control adjusts the cooling level through combining inlet temperature with garment flow rate modulation.

The system concept (Figure 1) for the liquid-cooled garment includes a circuit consisting basically of two flow loops. One loop includes the liquid-cooled garment (LCG) and the other a heat exchanger (HEX) for liquid cooling. If no fluid flows from the HEX loop to the LCG loop, then water present in the liquid-cooled garment is recirculated. In theory, its temperature will approach that of the skin of the astronaut. This corresponds to a zero-cooling-rate situation. Cooling rate is increased by allowing liquid to flow from the HEX loop into the LCG loop. Maximum cooling occurs when the crossover flow between the loops is equal to the flow through the heat exchanger.

Control signals which drive the temperature controller are produced within a fluid circuit, which acts essentially like a Wheatstone bridge. The umbilical, liquid-cooled garment, three-way valves, and orifice constitute a "garment circuit" which makes up one leg of the bridge. Resistance R_1, R_2, and R_3 form, respectively, the remaining three legs of the bridge. R_3 is adjustable to compensate for changes in umbilical flow resistance. Such compensation makes the system adaptable to a wide range of umbilical lengths. A change in cooling rate can be produced by varying a resistance located in the garment circuit.

Controller

The basic function of the fluidic temperature controller is to vary the ratio of warm fluid to cold fluid flowing to the liquid-cooled garment by responding to a relatively small pressure-difference signal generated in the bridge circuit (see Figure 1). The controller accepts the pressure signals at the bridge design levels and amplifies them to the magnitude required to modulate the mixing of warm and cold fluid.

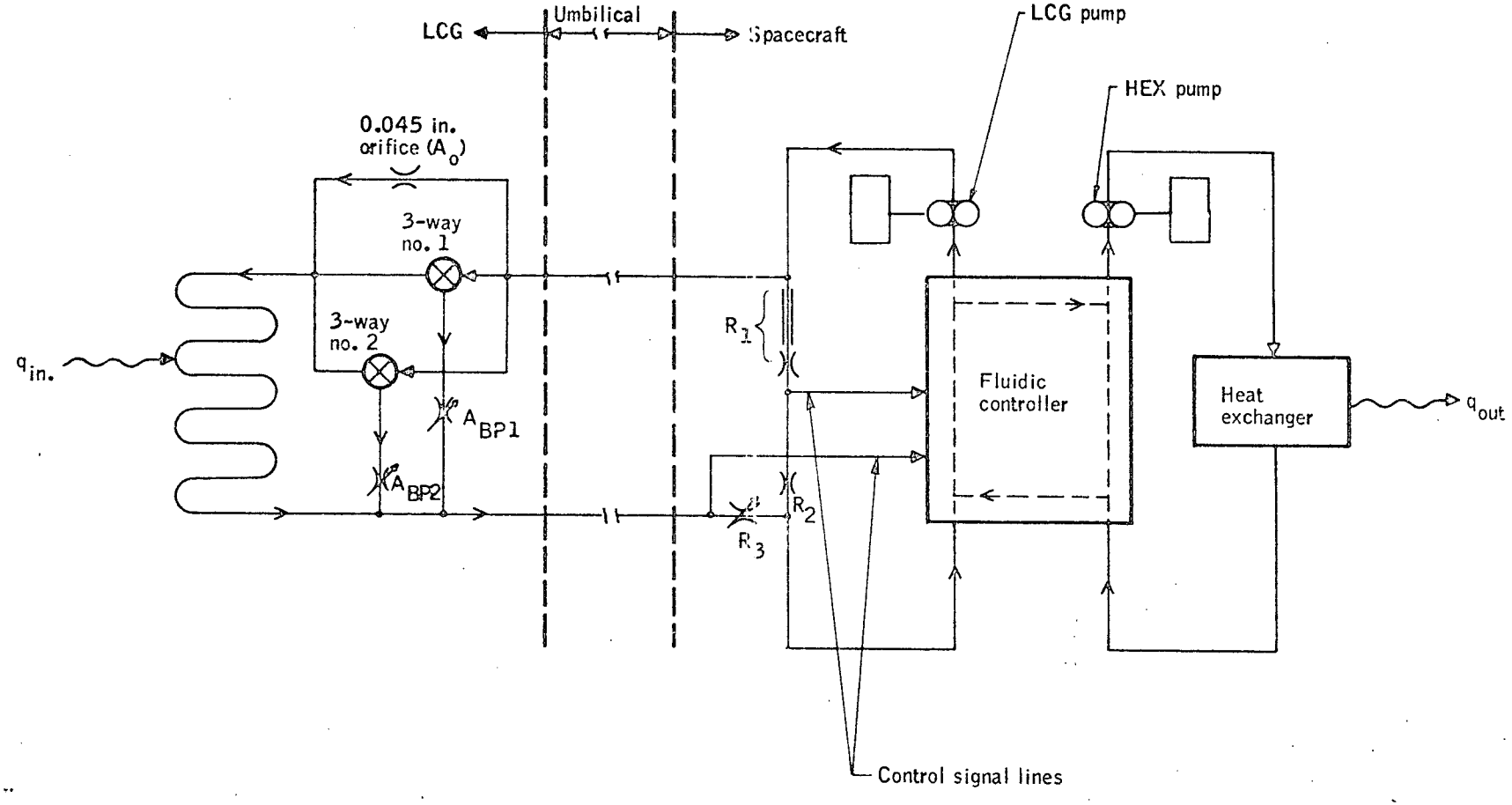

Figure 1. System Concept for Liquid-Cooled Garment

Figure 2 shows a photograph of the assembled temperature controller. A schematic of the controller circuit is shown in Figure 3. The controller consists of the following fluidic components:

- One 2-stage signal pressure level reducer
- Two 3-stage proportional amplifier cascades
- One mixing valve

In addition to these elements, the controller assembly incorporates three legs of the Wheatstone bridge.

The control pressure level reducer decreases control pressures to the controller and preserves control pressure difference. The proportional cascades provide controller sensitivity by amplifying both the pressure-difference signal generated by the bridge and the flow rate of the control fluid. The mixing valve modulates the warm and cold fluids, and provides on signal the desired mixing command from the proportional cascades. The fluidic mixing valve (Figure 4) is the key component of the controller.

Performance

The fluidic mixing valve produces a minimum mixing ratio of 0.10. With the mixing valve incorporated into the temperature controller, a system mixing ratio of 0.12 is obtained, which is equivalent to a cooling rate of about 750 BTU-hr. So that the subject is comfortable at rest (the subject having a metabolic rate of about 400 BTU/hr), a valve circuit throttles and bypasses flow to maintain sufficiently low cooling rates. The system provides a maximum garment inlet temperature of about 60° F.

MIXING VALVE FLOW PATTERNS

The main thrust in the controller refinement has been to optimize flow characteristics of the mixing valve. The procedure was basically an experimental approach using flow visualization techniques developed during this study. The actual viewing of flow patterns within the mixing valve provided the basis for valve modifications to expand its mixing ratio capability.

Flow patterns within the fluidic mixing valve depend primarily on the deflection of power jets. In Figure 5, flow patterns are indicated by arrows for the situation of zero jet deflection. This occurs, of course, when control pressures fed into the fluidic mixing valve are equal. The power jets from the two nozzles impinge against their respective splitters and are diverted partially to the LCG and partially to the heat exchanger. Hence, a zero jet deflection produces a mixture-ratio of 0.5.

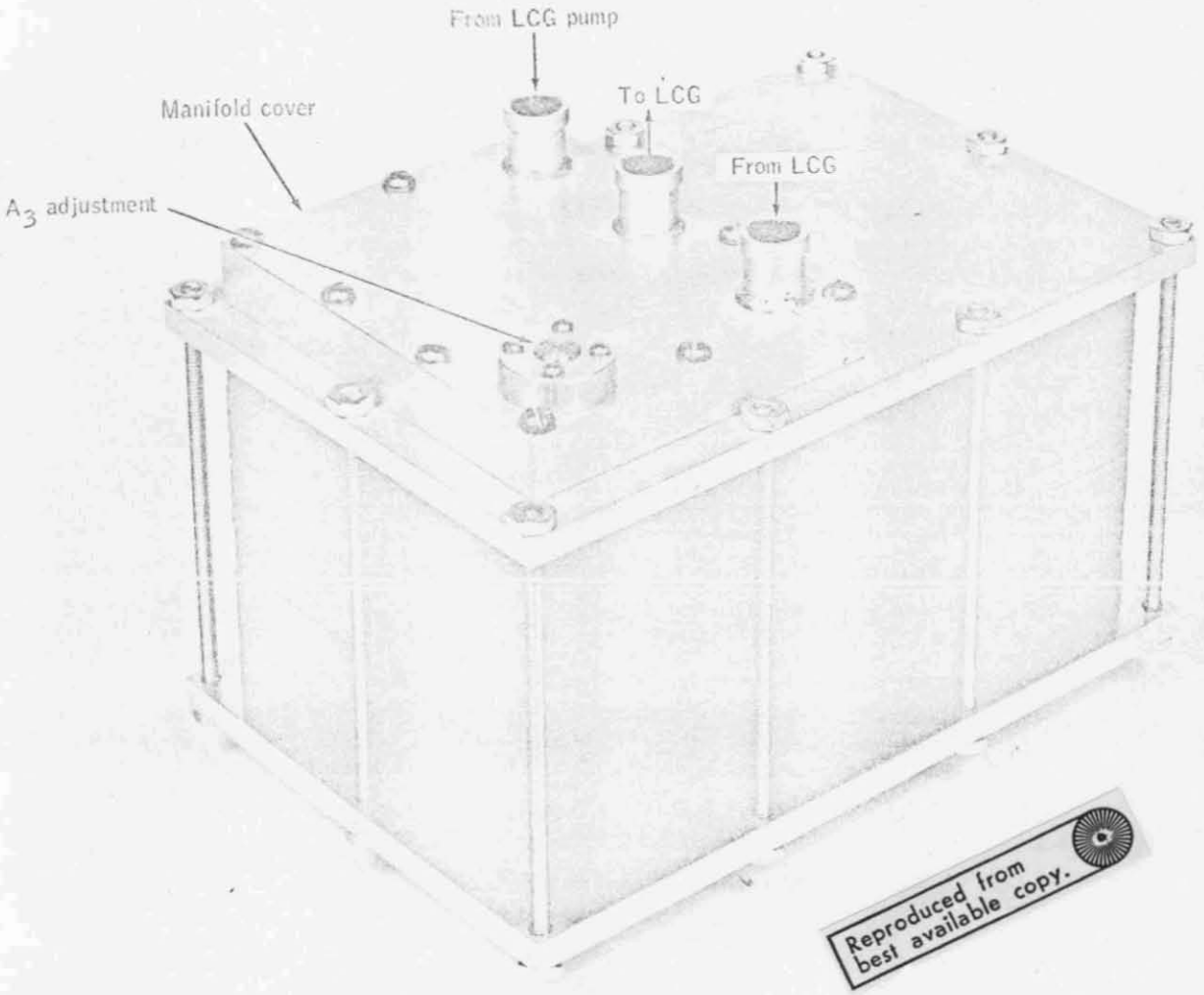

Figure 2. Assembled Controller - Top View

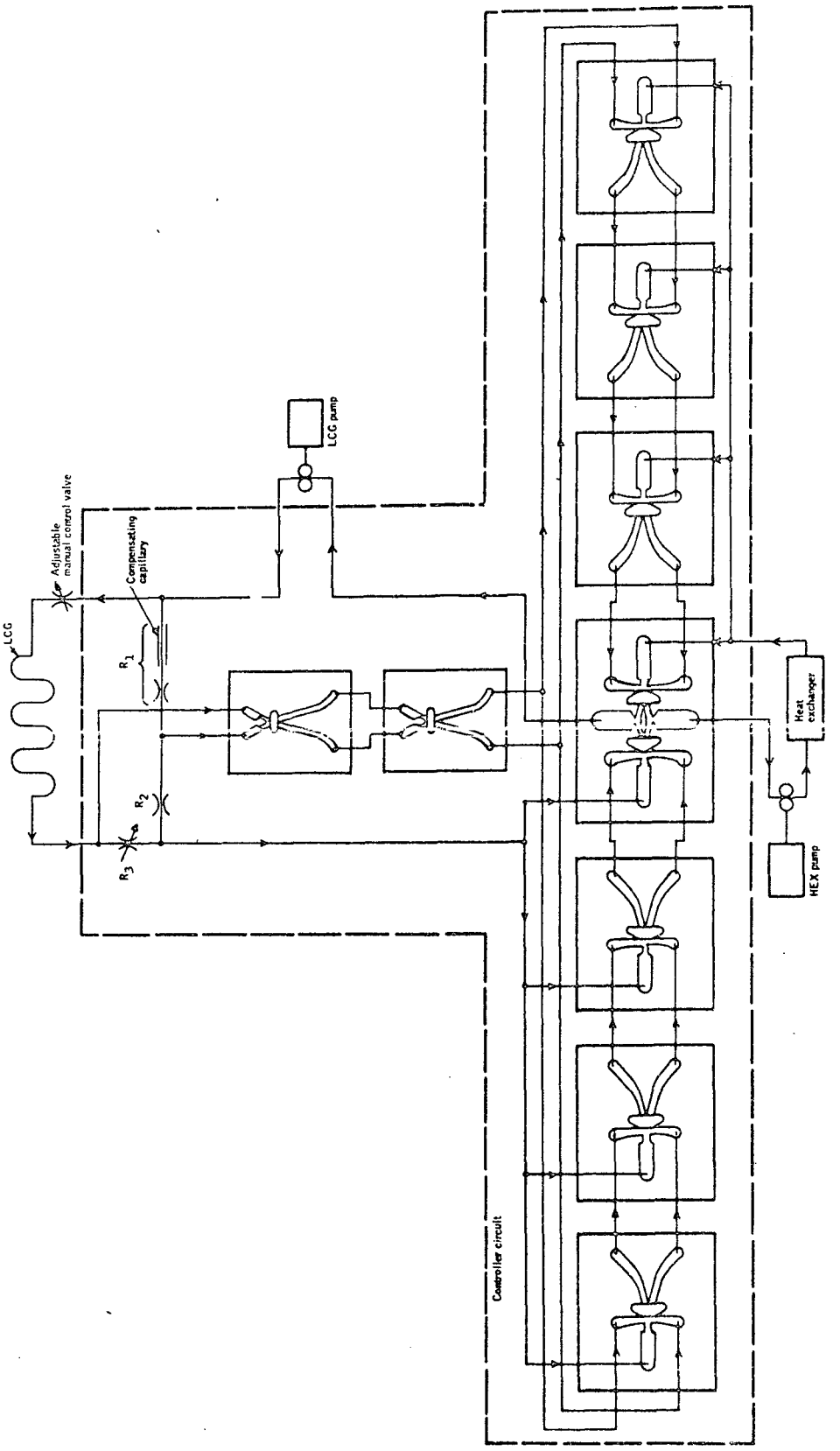

Figure 3. Controller Circuit

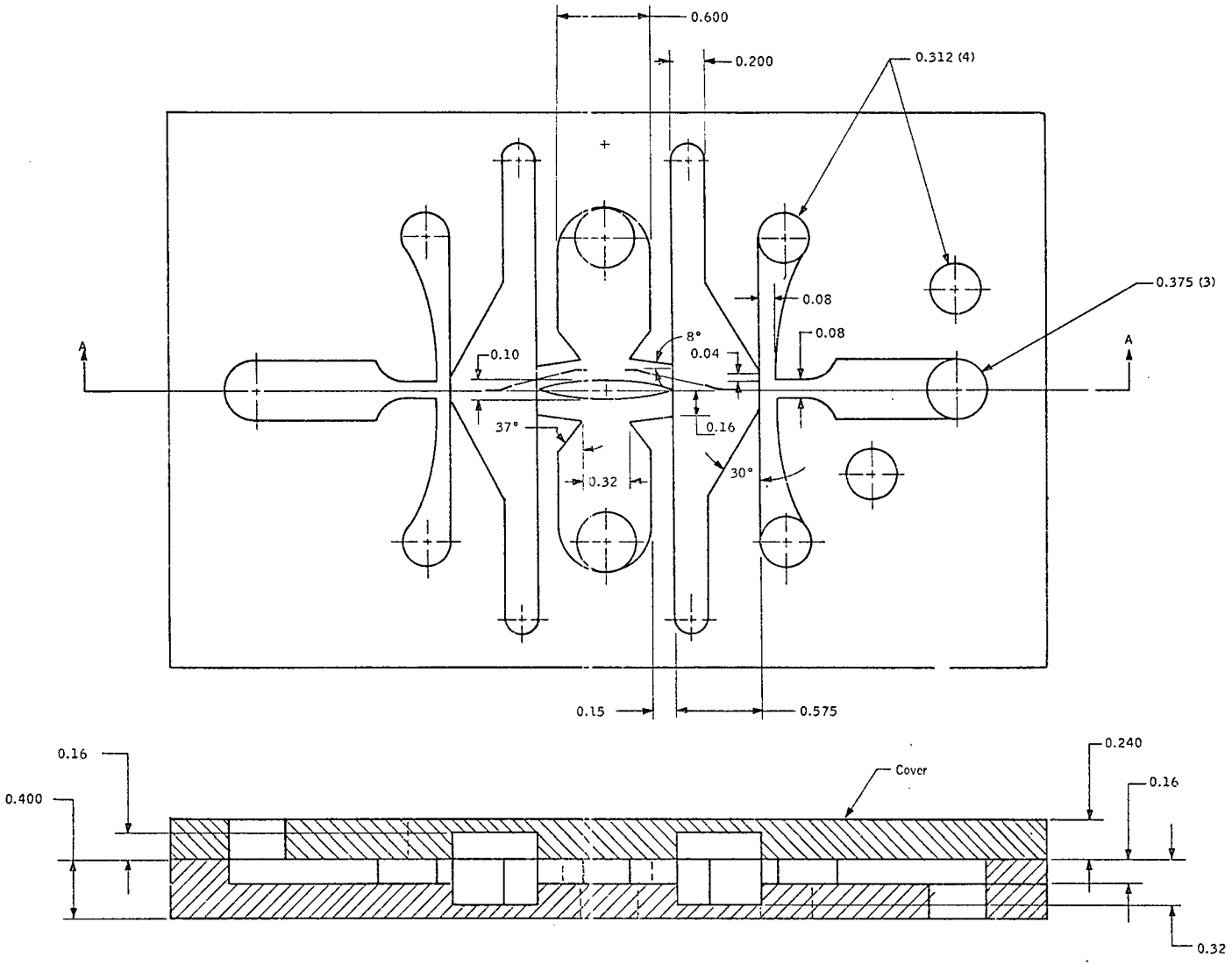

Figure 4. Component Dimensions - Fluidic Mixing Valve

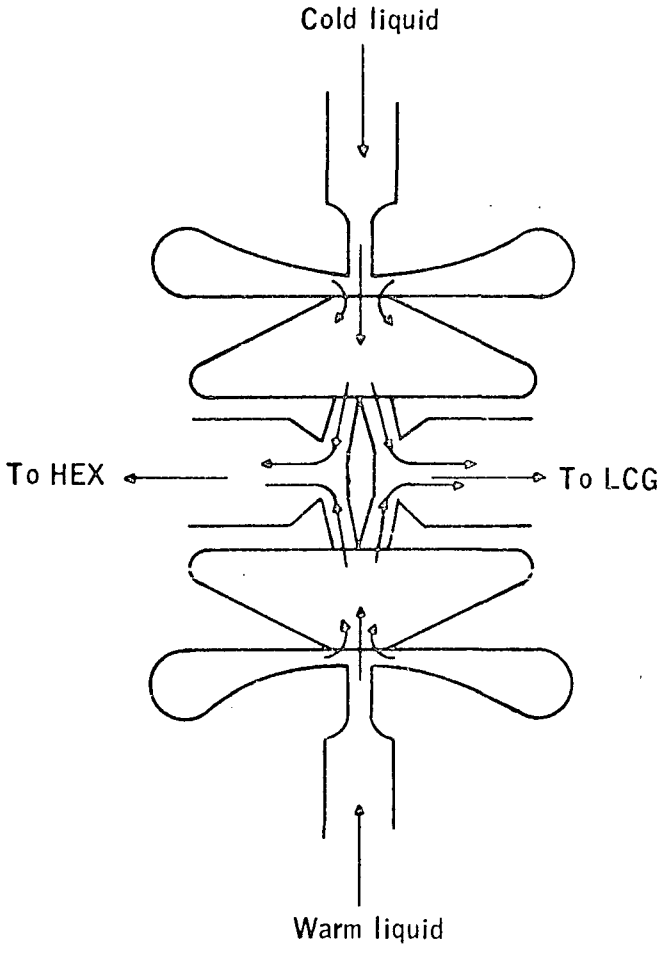

Figure 5. Flow Through the Fluidic Mixing Valve at Zero Jet Deflection

Deflecting the power jets in opposite directions produces extreme mixture ratios. Under this condition, one of three flow patterns may exist within the fluidic mixing valve. Ideally, a mixture ratio of either 0 or 1.0 calls for the flow pattern shown in Figure 6(b). Under this condition, the geometry of the device and the power jet deflections are such that a stagnant flow region, indicated by the shaded area, exists within the device. Only warm water flows to the LCG and only cold water to the heat exchanger. If this flow pattern could be produced within the controller, it would be easy to generate sufficiently low cooling rates to maintain a satisfactory thermal state. Thus, the flow pattern in Figure 6(b) does not exist within the fluidic mixing valve. More likely flow patterns are those of either Figure 6(a) or 6(c). Such patterns were of the type which resulted from the work done in the previous contract, as noted in Reference 1. For the pattern indicated in Figure 6(a), momentum differences within the device are high enough to cause the flow to move past the exit port and then recirculate around the opposite end of the splitter. In Figure 6(c), flow from one stream has insufficient momentum to stop the flow of fluid from an opposite direction. Flow conditions as defined by either Figures 6(a) or 6(c) could be eliminated through a proper selection of dimensions "A" or "B".

EXPERIMENTAL FLOW VISUALIZATION APPARATUS

The basic flow visualization technique uses near zero-buoyancy particles (polystyrene spheres) as tracers within the operating liquid (distilled water). These tracers indicate the flow patterns within the mixing valve and facilitate determining mixing ratio by permitting an actual particle count from the valve exits. During the flow visualization experiments, the mixing valve simulates its function in the temperature control circuit. Figure 7 illustrates the flow circuit of the experimental apparatus. The circuit simulates the heat exchanger by a filter which screens out the polystyrene spheres. This simulation permits the spheres to represent heat units. As the spheres are filtered by the simulated heat exchanger, they are recirculated into the warm loop. This recirculation simulates heat addition in the liquid-cooled garment. The experimental apparatus permits visualizing flow of the same sized mixing valve as that used in the temperature controller.

Polystyrene spheres are separated from exit flows in a specially designed reservoir. Both returns from the mixing valve are dumped in the hollow center cylinder housing the stirrer. The returned spheres are prevented from mixing with the simulated cold supply by a screen at the bottom of the center cylinder. The stirrer disperses the spheres to provide a simulated warm supply to one pump. Then, the returned liquid, without spheres, serves as the simulated cold supply to the other pump. The polystyrene spheres are sieved prior to entering the system to obtain a uniform size distribution. Sphere diameters range from 0.020 to 0.040 of an inch, which permits determining mixing ratios easily and accurately.

Figure 8 is a photograph of the mixing valve used in the experimental apparatus. The valve is a cast transparent epoxy model which permits illuminating the spheres in their flow patterns. Experimentation produced a lighting technique which makes the spheres highly visible; light is used which travels in

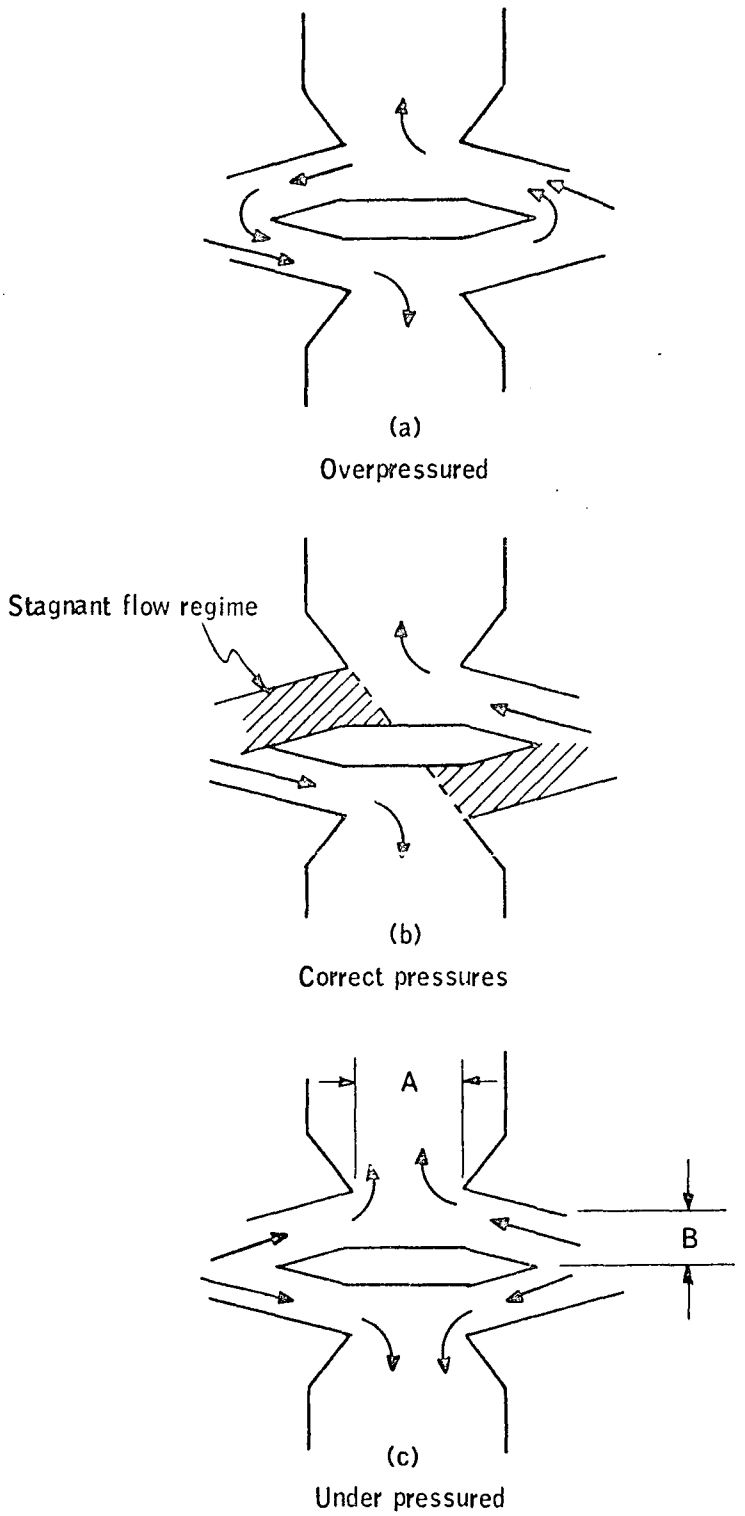

Figure 6. Possible Flow Patterns at Maximum Jet Deflection

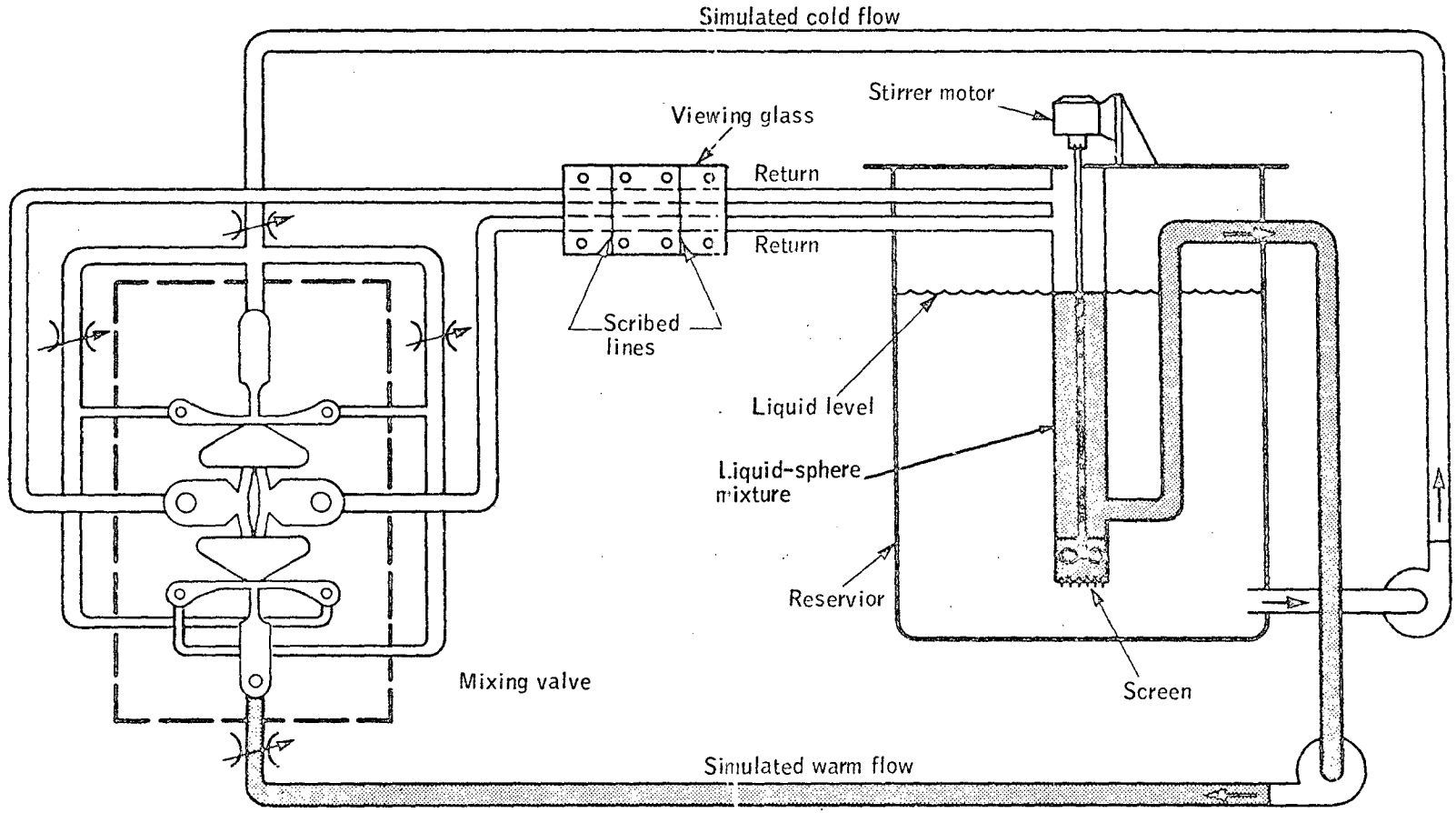

Figure 7. Flow Visualization Circuit for Mixing Valve Refinement

Figure 8. Fluidic Mixing Valve

the same plane as the flow, as well as perpendicular to the flow. The model is fitted with a clear transparent cover. All channels are blackened for contrast to facilitate visualization and photography. Ten pressure taps in the cover permit a continuous monitoring of pressure changes in the model as experimental investigations progresses. The mixing valve model is the same overall size as the one used in the temperature controller.

A viewing glass allows seeing the mixing ratio based on the spheres exiting from the experimental model. When the sphere-liquid mixture is homogenous, the procedure is to count the number of particles in each channel between scribed lines. The mixing ratio is determined by dividing the number of spheres in one channel by the total number in both channels. At mixing ratios near zero and one, the particles are counted over a given time interval. This is necessary since the sphere spacing in the low density channel may be such that no spheres would appear during the photographic time interval. In practice, the mixture is non-homogenous; therefore, a number of photographs are taken and averaged. Three exposures are taken on one frame which essentially increases the number of spheres between the scribed lines. Figure 9 is a photograph showing the results of strobing the viewing glass three times. Note that the spheres are easily counted, and, thus the mixing ratio easily determined.

AREAS OF CONTROLLER REFINEMENT

Experimental studies reveal controller performance can be improved in several areas. A discussion and where possible an assessment of these areas are presented below.

Exit Vortices

As shown by the flow visualization apparatus, the mixing valve exit pressures fluctuated randomly during the experimental investigations. These fluctuations were attributed to vortex flow patterns being set up in the mixing valve exit passageways. Vortices were eliminated by installing flow straighteners in each exit of the mixing valve.

Geometry Optimizing

The flow visualization experiments were conducted on an adjustable, mixing valve model. To fully concentrate effort on mixing valve optimization, neither proportional amplifier cascade was included in the visualization studies. Eighteen different valve configurations were tested, including the original design. Table 1 presents the configuration dimensions tested and the mixing ratio experimentally obtained for each case. Figure 10 defines the dimensions A, B, and C used in the table. The best configuration tested (run Number 8, having a mixing ratio of 0.04) was refined further by investigating the effects of small perturbations of dimension B and by rounding all corners on the upstream edges of the receiver legs. Figure 10 also shows the locations of the added radii refinements. These refinements improved the minimum mixing ratio to 0.03. The optimum mixing valve dimensions are:

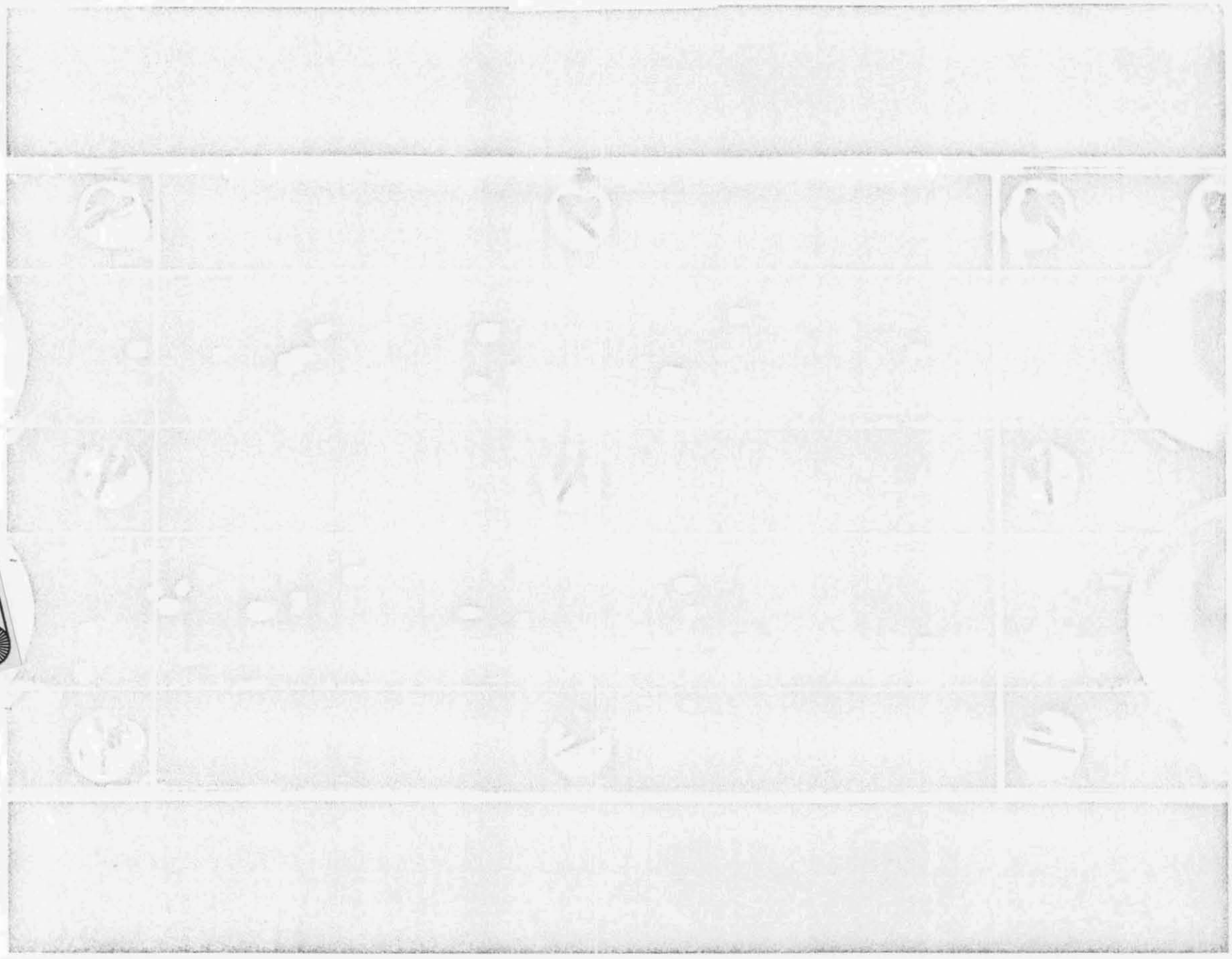

Figure 9. Viewing Glass, Photographed Three Times, Facilitates Counting Spheres

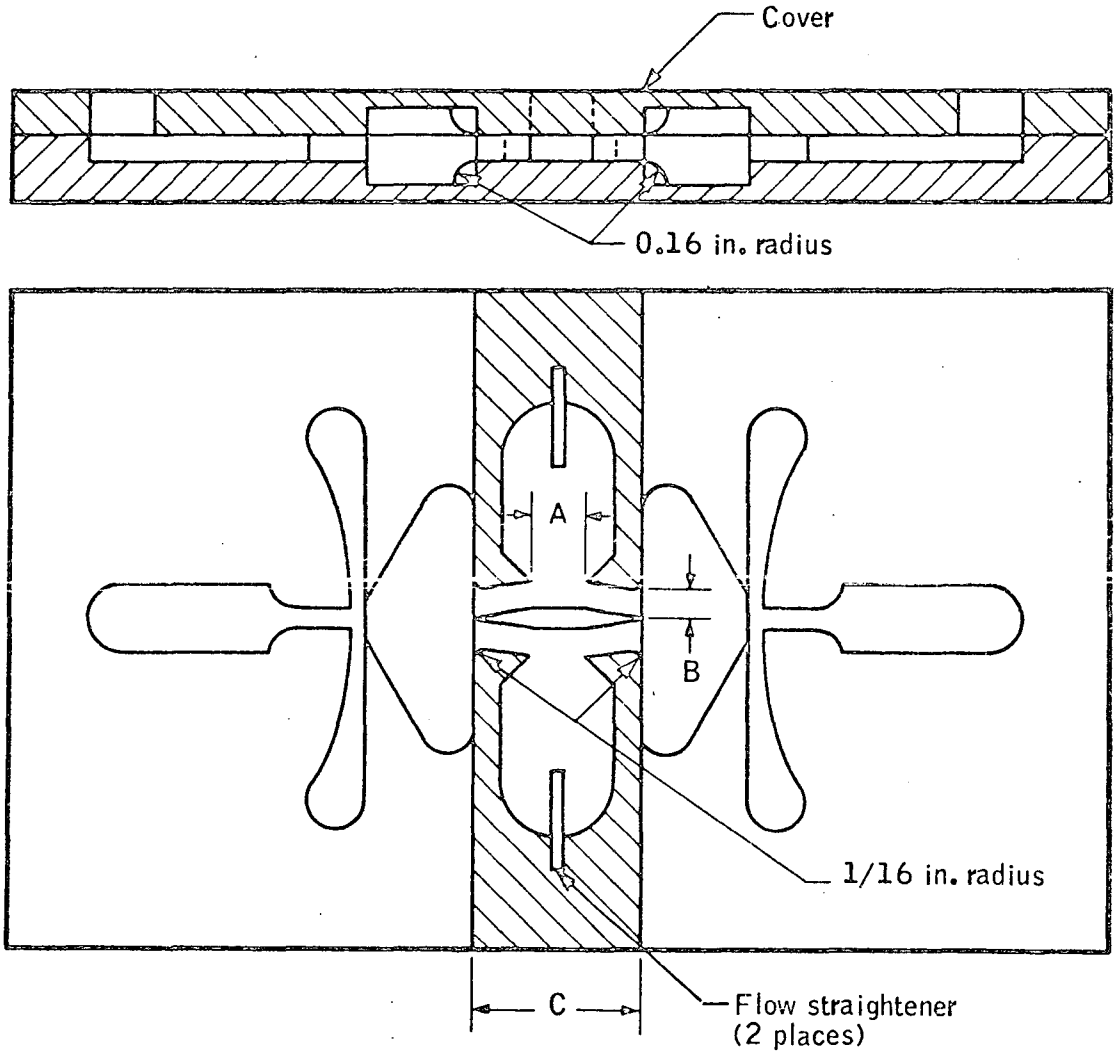

Figure 10. Variable Geometry Fluidic Mixing Valve

TABLE 1. - VISUALIZATION TEST RUNS

Run Number	Valve Dimensions, In. *			Mixing Ratio
	A	B	C	
1	0.32	0.24	0.90	0.22
2 (orig.)	0.32	0.16	0.90	0.07
3	0.32	0.11	0.90	0.27
4	0.48	0.24	0.90	0.22
5	0.48	0.16	0.90	0.08
6	0.48	0.11	0.90	0.24
7	0.21	0.24	0.90	0.27
8	0.21	0.16	0.90	0.04
9	0.21	0.11	0.90	0.26
10	0.32	0.24	1.10	0.21
11	0.32	0.16	1.10	0.08
12	0.32	0.11	1.10	0.24
13	0.48	0.24	1.10	0.21
14	0.48	0.16	1.10	0.07
15	0.48	0.11	1.10	0.25
16	0.21	0.24	1.10	0.20
17	0.21	0.16	1.10	0.05
18	0.21	0.11	1.10	0.28

* See Figure 10

A = 0.21 inch

B = 0.14 inch

C = 0.90 inch

The original valve shown in Table 1, Run Number 2, has a mixing ratio of 0.07.

Amplifier Noise

The optimized mixing valve having a mixing ratio of 0.03 was bench tested with the proportional cascades in the circuit. The performance degraded to a mixing ratio of 0.06. Experiments showed degradation was due to noise generated by the cascades. An analysis of noise dampening plenums (see Appendix A) resulted in incorporating plenum chambers in the control lines between the proportional cascades and the mixing valve. By adding the plenums, the mixing ratio, as determined by flow visualization techniques, improved to 0.03 again. The four plenum chambers permit a minimum disruption when incorporated into the basic controller design. Two additional layers, each having two plenums, are added to the controller stack (Figure 11). In conditions of zero gravity, thin flexible air bag containers could be incorporated inside each plenum chamber to maintain a gas-water interface.

Heat Transfer

All flow visualization experiments were conducted with essentially a constant-temperature liquid. When the optimized mixing valve was operated with a cold water supply and the liquid-cooled garmet heated by a radiant heater, the performance (based on temperature measurement) degraded to a mixing ratio of 0.08. To verify that a portion of the degradation was due to heat transfer through the valve material, a simple experimental test was conducted. The mixing valve receiver channels were blocked in two places (Figure 12) to eliminate mixing the cold and warm water. The cold water entered the valve and exited without mixing with the warm water. A pseudo-mixing ratio was gotten of 0.014, based on temperature measurements. This indicated that the valve material formed a conduction path between the two thermally different liquids, thereby creating the pseudo-mixing ratio. To lower the "thermal short" between the warm and cold liquids, thermal-barriers (air gaps) are incorporated in the mixing valve body.

Flow Balancing

Since the conductive heat transfer accounted for about 0.014 degradation of the mixing ratio, other experimental techniques were explored to ascertain why the performance had degraded. A flow balancing procedure was pursued by incorporating a vent in the cold interaction region of the mixing valve and routing the vent flow to the cold exit. For testing flexibility, another vent was incorporated in the warm interaction region to the warm exit. The mixing valve, when tested for performance based on temperature measurement,

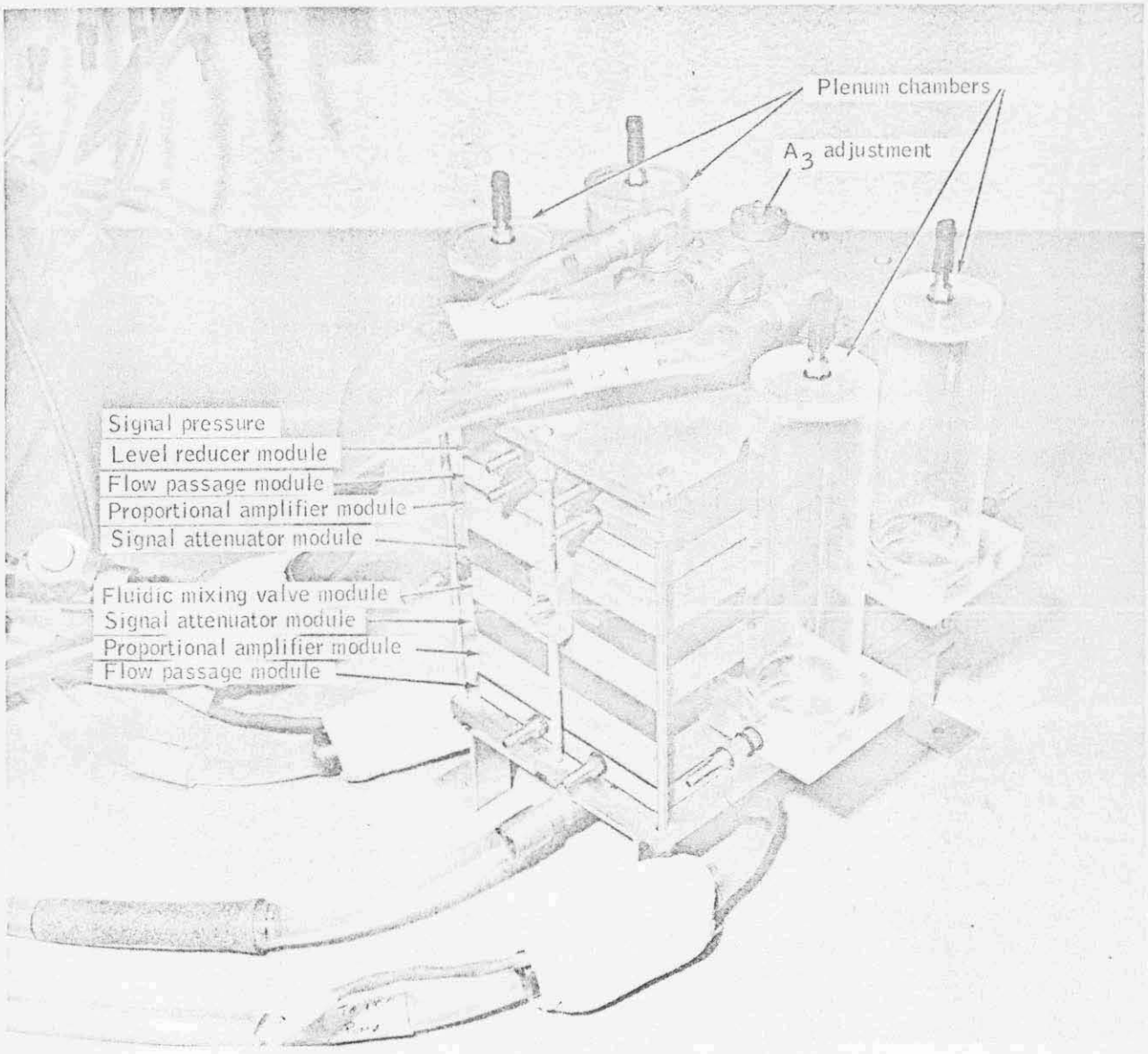

Figure 11. Improved Controller Stack

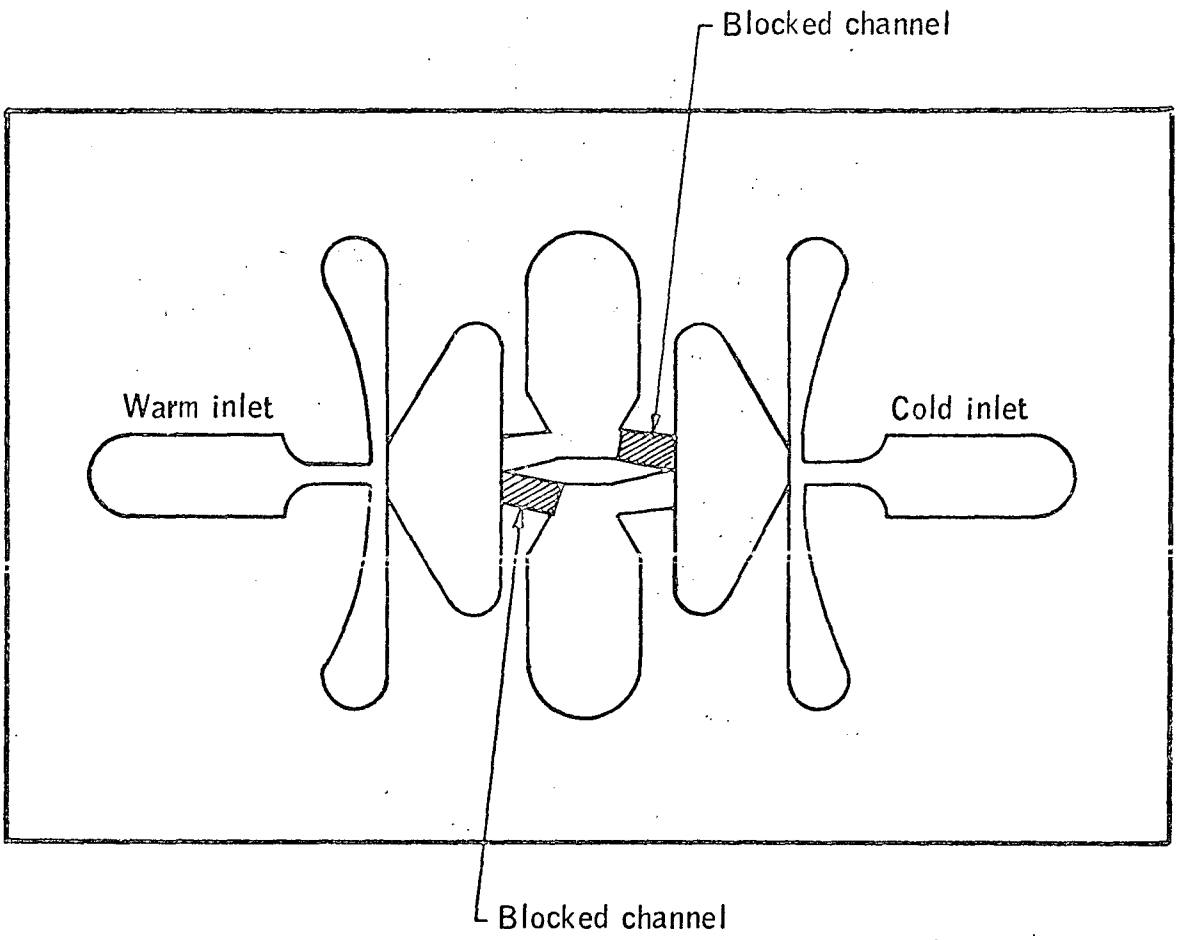

Figure 12. Mixing Valve with Blocked Channels

produced a pseudo-mixing ratio of 0.05. The best performance occurred with 10 percent of the cold flow vented, the warm vent closed, and the cold supply flow about 10 percent greater than the warm supply flow rate.

MANUAL CONTROL VALVE

The manual control valve (Figure 13) on the garment adjusts the cooling rate through temperature modulation. No flow is bypassed, and the flow rate through the garmet remains unchanged. A valve indicator plate displays three major valve settings: warm; medium; and cold. The one valve, infinitely variable over the range displayed on the plate, replaces the flow-diverting valving system which modulated flow rate to the garment. An improved system concept incorporating the adjustable manual control valve is shown in Figure 14.

SYSTEM OPERATION

Garment inlet temperatures are varied by changing the flow resistance through the previously described manual control valve. Closing the valve reduces PCR1, the control pressure at one inlet port of the pressure level reducer, with respect to PCR2, the control pressure at the other reducer inlet port. The net result is increased mixing between the LCG and HEX loops and a lower garment inlet temperature.

Experimental characterization of the system is represented by the data in Figure 15. These data indicate that maximum cooling occurs for PCR2 = PCR1, moderate cooling for a differential of 0.25 inch of water, and minimum cooling for pressure difference in excess of 0.5 inch of water. The minimum garment inlet temperature is 2°F above cold supply temperature. Maximum inlet temperature is 28.5°F above cold supply temperature.

Pressure differences produced by the "W", "M", and "C" positions of the manual control valve are indicated in Figure 15. These data are for a 50 ft umbilical with 3/8 in. I.D. liquid conduits.

For umbilicals of shorter or longer length, adjustments can be made to achieve the same sensitivity of garmet inlet temperature to change in valve flow area. The relations between temperature and control pressure difference (see Figure 15) are independent of umbilical length. Hence, the desired sensitivity is achieved if the "W", "M" and "C" setting correspond to the pressure differences indicated in the figure. A pressure difference of zero at the "C" setting is readily obtained through adjusting A_3 on the face of the controller (see Figure 11). The pressure difference produced at the "W" setting depends on the fractional change in flow resistance in the garment circuit produced by going from the "C" to "W" setting, hence, an increase in pressure difference at the "W" setting results from the "C" setting (and zero pressure difference) occurring at a smaller flow area through the valve and vice versa. The dial on the valve shown in Figure 13 is adjustable to facilitate corresponding the flow area with the "C" setting.

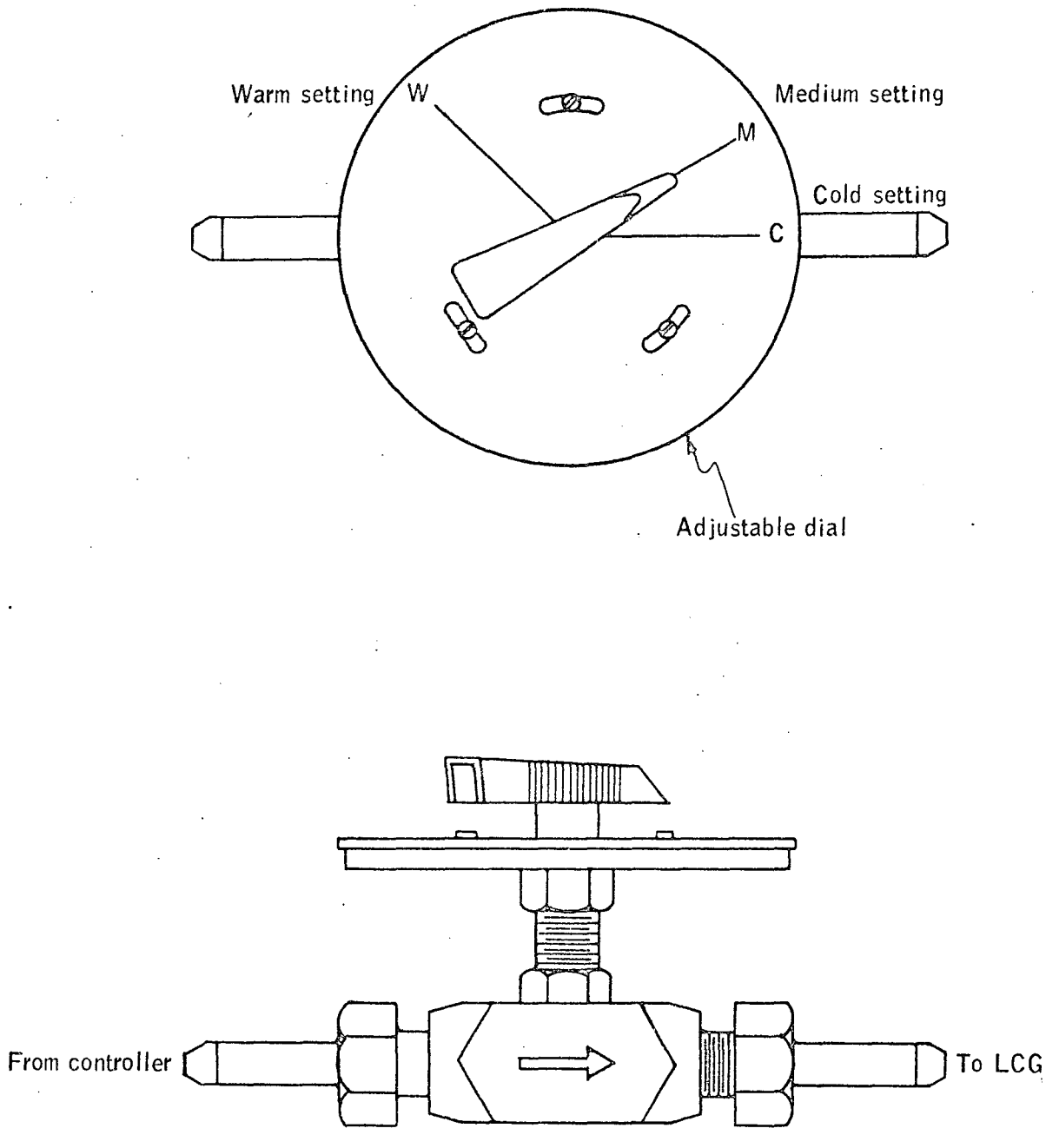

Figure 13. Manual Control Valve

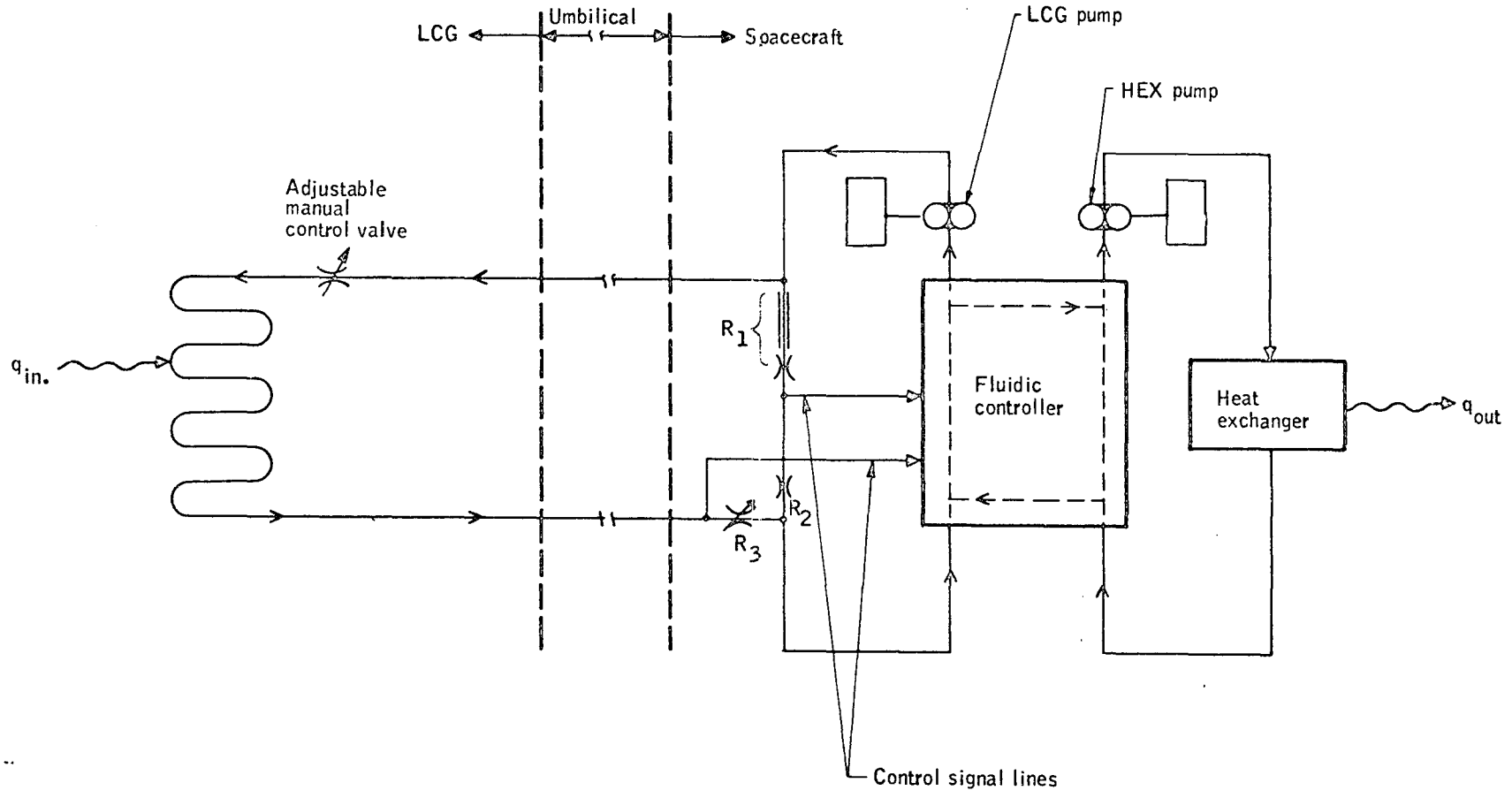

Figure 14. Improved System Concept for Liquid-Cooled Garment

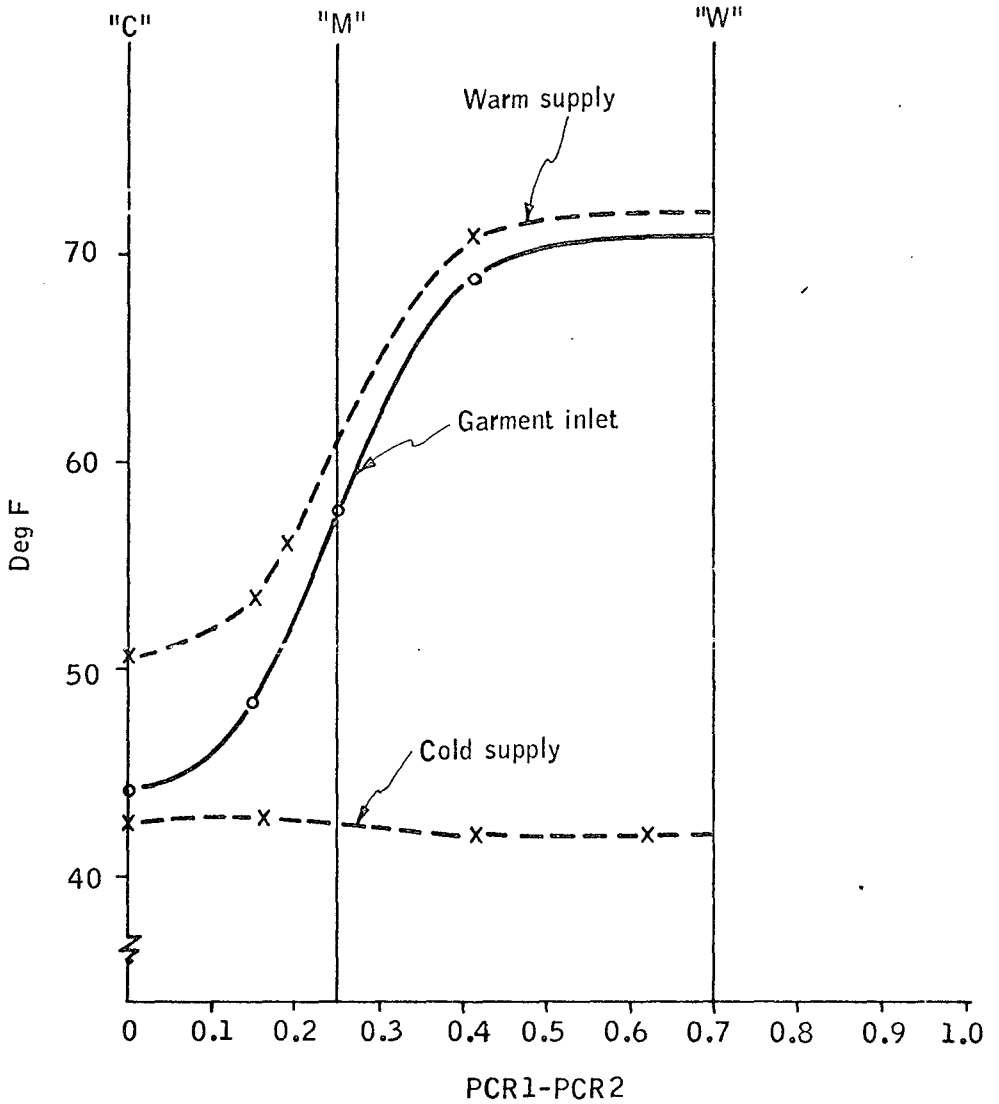

Figure 15. Temperature Variation versus Control Pressure Difference

CONCLUSIONS

1. A refined fluidic temperature controller can regulate garment inlet temperatures from 45°F to 70°F without using external heat sources.

2. Simulated mixture ratios, based on temperature measurements, as low as 0.074, can be produced by the fluidic controller. This residual mixing ratio is a sum of the following contributions:

• Physical mixing:	0.030
• Heat transfer:	0.014
• Control flow interchange between HEX and LCG loop	0.030
Total	0.074

3. Modulating inlet temperature can be achieved by a single valve in series with the LCG. No bypassing or changing of garment flow is required.

APPENDIX A
ATTENUATION OF PRESSURE FLUCTUATION

Attenuating pressure fluctuation in a liquid system requires introducing a compressible medium, such as air, in a plenum-type device (see Figure A1). The device receives a time-dependent pressure signal, P_S, and produces pressure, P_C, with fluctuations in time that are greatly attenuated. Extent of attenuation can be estimated from the formulae derived in the following analysis.

Assume that pressures can be divided into average and time-varying components, i.e.

$$P_c = \bar{P}_c + \delta P_c$$

$$P_s = \bar{P}_s + \delta P_s$$

where δP_S and δP_C are considerably less than $\bar{P}_S$ and $\bar{P}_C$, respectively. Further assume that the plenum pressure, P_P, is essentially constant and equal to $\bar{P}_C$. Fluctuations in P_C will, thus, cause the slug of fluid of length, L, cross-sectional area, A, and density, ρ, to accelerate at a rate given by

$$\ddot{x} = \frac{(P_c - P_P)A}{\rho L A}$$

$$= \frac{\delta P_c}{\rho L} \qquad \text{(A1)}$$

By continuity,

$$\dot{m}_s - \dot{m}_c = \rho \dot{x} A \qquad \text{(A2)}$$

or

$$A_s\sqrt{2\rho (P_s - P_c)} - A_c\sqrt{2\rho P_c} = \rho \dot{x} A \qquad \text{(A3)}$$

However, since the δP's are much less than the $\bar{P}$'s,

$$A_s\sqrt{2\rho (\bar{P}_s - \bar{P}_c)}\left[1 + \frac{1}{2}\frac{\delta P_s - \delta P_c}{\bar{P}_s - \bar{P}_c}\right]$$

$$- A_c\sqrt{2\rho \bar{P}_c}\left[1 + \frac{1}{2}\frac{\delta P_c}{\bar{P}_c}\right] = \rho \dot{x} A \qquad \text{(A4)}$$

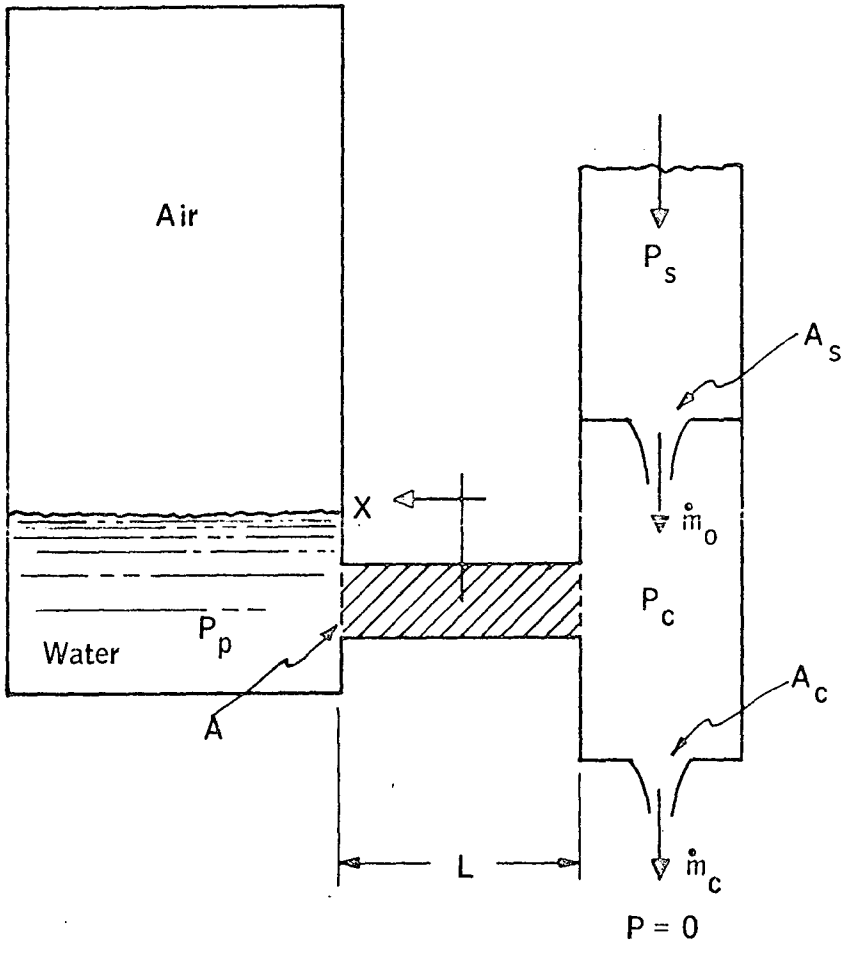

Figure A1. Schematic of Damper

The terms $A_s\sqrt{2\rho(\bar{P}_s-\bar{P}_c)}$ and $A_c\sqrt{2\rho\,\bar{P}_c}$ are approximate time-averaged flow rates, and must, therefore, be equal. Thus, (A4) becomes, after some rearrangement,

$$A_s^{\,2}\,(\delta P_s - \delta P_c) - A_c^{\,2}\,\delta P_c = \dot{m}\,\dot{x}\,A \tag{A5}$$

where

$$\dot{m} = \bar{\dot{m}}_c = \bar{\dot{m}}_s$$

Differentiating (A5) and combining with (A1) results in the equation

$$\frac{d(\delta P_c)}{dt} + \frac{\dot{m}\,A}{\rho L(A_s^{\,2} + A_c^{\,2})}\,\delta P_c = \frac{A_s^{\,2}}{A_c^{\,2} + A_s^{\,2}}\,\frac{d(\delta P_s)}{dt} \tag{A6}$$

For $\delta P_s = |\delta P_s|\cos\omega t$, the steady state solution for (A6) is

$$\delta P_c = \frac{R\,|\delta P_s|\,\omega}{\omega^2 + (1/\tau)^2}\left(\frac{1}{\tau}\cos\omega t + \omega\sin\omega t\right) \tag{A7}$$

where

$$R = \frac{A_s^{\,2}}{A_c^{\,2} + A_s^{\,2}} \tag{A8}$$

and

$$\tau = \frac{\rho L(A_s^{\,2} + A_c^{\,2})}{\dot{m}A} \tag{A9}$$

An amplitude attenuation factor M is given

$$M = \frac{|\delta P_c|}{|\delta P_s|} = \frac{R}{\sqrt{1 + \frac{1}{\tau^2\omega^2}}} \tag{A10}$$

Increasing attenuation thus results from decreasing R and decreasing τ. This is accomplished for a given ω by

- Decreasing A_s with respect to A_c
- Decreasing L
- Increasing A

The damping plenums used in the fluidic controller have the following approximate dimensions and operating conditions:

ρ = 1.94 slugs/cu ft

A = 0.25 in.^{2}

$L \cong$ 1 in.

$\dot{m}$ = 48 lb per hr

A_c = 0.0048 in.^{2}

A_s = 0.0123 in.^{2}

These conditions result in τ = 0.0019 sec and R = 0.87. The amplitude attenuation factor for several values of $\omega/2\pi$ is given in Table A-1. These data indicate that the plenums will effectively attenuate fluctuations at frequencies under 10 cps.

TABLE A-1. - AMPLITUDE ATTENUATION BY DAMPING PLENUMS

$\frac{\omega}{2\pi}$	M
1	0.0103
10	0.092
100	0.656

REFERENCES

1. Starr, J. B.; and Merrill, G. L.: Fluidic Temperature Control System for Liquid Cooled Space Suits. Report No. 12128-FR1 (Contract No. NAS 9-8249) National Aeronautics and Space Administration, Manned Spacecraft Center, Houston, Texas.

2. Starr, J. B.; and Merrill, G. L.: Fluidic Temperature Control for Liquid-Cooled Flight Suits. Report No. NADC-AC-6818, Naval Air Development Center, Johnsville, Pa.

3. Eckert, E. R. G.; and Drake, R. M.: Heat and Mass Transfer, Second ed., Chp. 17, McGraw-Hill Book Co., Inc. 1959.